Proteasome inhibitor MG132 enhances the sensitivity of human OSCC cells to cisplatin via a ROS/DNA damage/p53 axis

ZHENG ZHENG, XIANG WANG and DONGLEI CHEN

Department of Stomatology, The First People's Hospital of Nantong, Affiliated Hospital 2 of Nantong University, Nantong, Jiangsu 226000, P.R. China

Received October 2, 2022; Accepted February 27, 2023

DOI: 10.3892/etm.2023.11924

Abstract. Cis-diamine-dichloroplatinum II (cisplatin, CDDP) is a key chemotherapeutic regimen in the treatment of oral squamous cell carcinoma (OSCC). However, the therapeutic efficacy of cisplatin in OSCC may be hampered by chemoresistance. Therefore, the development of novel combination therapy strategies to overcome the limitations of CDDP is of great importance. The proteasome inhibitor MG132 exhibits anti-cancer properties against various types of cancer. However, our knowledge of its anti-cancer effects in combination with CDDP in OSCC cells remains limited. In the current study, the synergetic effects of MG132 and CDDP were evaluated in the human CAL27 OSCC cell line. CAL27 cells were treated with CDDP alone or in combination with MG132. The results showed that MG132 significantly reduced cell viability in a dose-dependent manner. Additionally, cell viability was significantly reduced in CAL27 cells treated with 0.2 μM MG132 and 2 μM CDDP compared with cells treated with MG132 or CDDP alone. In addition, MG132 significantly enhanced the CDDP-induced generation of intracellular reactive oxygen species and DNA damage in OSCC cells. Furthermore, treatment with CDDP or MG132 alone notably inhibited colony formation and proliferation of OSCC cells. However, co-treatment of OSCC cells with MG132 and CDDP further hampered colony formation and proliferation compared with cells treated with either MG132 or CDDP alone. Finally, in cells co-treated with MG132 and CDDP, the expression of p53 was markedly elevated and the p53-mediated apoptotic pathway was further activated compared with cells treated with MG132 or CDDP alone, as shown by the enhanced cell apoptosis, Bax upregulation, and Bcl-2 downregulation. Overall, the results of the current study support the synergistic anti-cancer effects of a combination of MG132 and CDDP against OSCC, thus suggesting that the combination of MG132 and CDDP may be a promising therapeutic strategy for the management of OSCC.

Correspondence to: Dr Donglei Chen or Dr Xiang Wang, Department of Stomatology, The First People's Hospital of Nantong, Affiliated Hospital 2 of Nantong University, 6 Haierxiang Road, Nantong, Jiangsu 226000, P.R. China
E-mail: cdl78780@126.com
E-mail: dentistw@qq.com

Key words: cisplatin, MG132, oral squamous cell carcinoma, chemosensitivity

Introduction

Oral cancer is the 16th most common type of cancer worldwide, and oral squamous cell carcinoma (OSCC) accounts for ~90% of all oral cancer cases (1). OSCC is a multifactorial disease that arises from the stratified squamous epithelium in the oral mucosa (2,3). Surgical resection of the primary tumor combined with radiotherapy and chemotherapy is the most common treatment approach for advanced OSCC (4). However, cis-diamine-dichloroplatinum II (cisplatin, CDDP) chemoresistance often results in treatment failure and a poor prognosis (5), with a 5-year survival rate of <50% for patients with advanced OSCC (6). Therefore, developing effective adjuvant treatment approaches to increase drug sensitivity to complement current therapeutics and improve overall survival is of great significance.

The ubiquitin-proteasome pathway is a major intracellular pathway involved in protein degradation. Numerous fundamental cellular processes depend on the ubiquitin-proteasome pathway, including cell cycle, cell apoptosis, and cell differentiation (7-9). Additionally, the ubiquitin-proteasome pathway has been extensively studied in cancer therapy (10,11). A previous study showed that the proteasome inhibitor MG132 (carbobenzoxy-L-leucyl-L-leucyl-L-leucinal) could effectively inhibit the proteolytic activity of the 26S proteasome complex (12). It has been also reported that MG132 exerts therapeutic effects in several types of cancer, such as lung cancer, and hypopharyngeal cancer (13,14). Furthermore, MG132 also increases the sensitivity of ovarian carcinoma and esophageal squamous cell carcinoma cells to chemotherapeutic drugs (15,16). Although MG132 has been reported to affect CDDP sensitivity in oral cancer, and the underlying molecular mechanism involved has been partly explored (17-19), further research is required to investigate the in-depth mechanism underlying MG132 induced CDDP sensitivity in oral cancer.

In the current study, OSCC cells were co-treated with MG132 and CDDP to evaluate the effect of MG132 on cell

viability, cell proliferation, apoptosis, and intracellular reactive oxygen species (ROS) generation. Furthermore, the effect of MG132 on the p53-mediated apoptotic signaling pathway in CDDP-treated OSCC cells was determined.

Materials and methods

Cell culture and morphology. The human CAL27 OSCC cell line was a kind gift from the Nanjing Stomatological Hospital. CAL27 cells were cultured in high glucose DMEM (Wisent, Inc.) supplemented with 10% FBS (Gibco; Thermo Fisher Scientific, Inc.), 100 units/ml penicillin G, and 100 μg/ml streptomycin in a humidified incubator supplied with 5% CO_2 at 37˚C. When cells reached confluency, cells were treated with trypsin to detach them and split or used as required. The morphology of CAL27 cells treated with PBS (control cells), 0.2 μM MG132 (MedChemExpress), and/or 2 μM CDDP (MedChemExpress) for 48 h was directly observed using an Olympus inverted bright-field light microscope CKX41 (Olympus Corporation; magnification, x40).

Cell viability. Cells were seeded into 96-well plates at a density of $5x10^3$ cells/well and cultured overnight at 37˚C in a 5% CO_2 incubator. Following treatment with CDDP, MG132, or a combination of both for 48 h, each well of the 96-well plate was treated with 10 μl Cell Counting Kit 8 (CCK-8) solution (Beyotime Institute of Biotechnology), and cells were further incubated for 4 h. The absorbance at a wavelength of 450 nm was measured using a Varioskan LUX microplate reader (Thermo Fisher Scientific, Inc.).

Measurement of ROS. The intracellular ROS levels were quantified using an ROS assay kit (Beyotime Institute of Biotechnology). Following treatment with CDDP and/or MG132, cells were harvested and incubated with 10 μM DCFH-DA probe for 20 min at 37˚C. The labeled cells were then washed twice with PBS and counted using a flow cytometer (Beckman Coulter) at excitation and emission wavelengths of 488 and 525 nm.

TUNEL assay. TUNEL assays were performed according to the manufacturer's instructions. Briefly, cells were treated with PBS (control), CDDP, MG132, or CDDP + MG132 for 48 h. Cells were then fixed with 4% polyformaldehyde (Sinopharm Chemical Reagent Co., Ltd.) for 30 min at room temperature (RT), permeabilized with 0.3% Triton X-100 (Sinopharm), and incubated with TUNEL detection solution (Beyotime Institute of Biotechnology) for 1 h at 37˚C. Following cell staining with Hoechst 33342 for 10 min at RT (Beyotime Institute of Biotechnology), images were captured using a Leica fluorescence microscope DMi8 (Leica Biosystems; magnification, x200).

Colony formation assay. A colony formation assay was performed to evaluate the proliferation potential of OSCC cells. Briefly, cells were seeded into 6-well plates at a density of $1x10^3$ cells/well and allowed to adhere overnight. Subsequently, cells were treated with PBS, CDDP, MG132, or CDDP + MG132 and cultured for up to 7 days. Following fixing with methanol for 30 min at RT, the colonies were stained with 0.1% crystal violet (Sinopharm) solution for 30 min at RT. Colonies consisting of >20 cells were included in the analysis.

Ethynyl-2-deoxyuridine (EdU) assay. Cell proliferation was assessed using an EdU staining using the BeyoClick EdU kit (Beyotime Institute of Biotechnology), according to the manufacturer's protocol. Briefly, cells were treated with PBS, CDDP, MG132, or CDDP + MG132 for 48 h and were then incubated with 10 μM EdU at 37˚C for an additional 2 h. Following washing with PBS, cells were fixed with 4% polyformaldehyde at RT, permeabilized with 0.3 Triton X-100 followed by incubation with Click additive solution (Beyotime Institute of Biotechnology) at RT for 30 min in the dark. After staining with EdU, cells were counterstained with Hoechst 33342 for 10 min at RT and observed under a Leica fluorescence microscope DMi8 (Leica Biosystems; magnification, x200).

Annexin-V apoptosis detection assay. To assess cell apoptosis, cells were treated with CDDP and/or MG132 for 48 h. Following trypsinization, cells were incubated with an annexin V-FITC binding buffer containing annexin V-FITC (Vazyme Biotechnology Co. Ltd.), and propidium iodide (PI) at RT for 10 min. Following staining, cells were sorted using a DxFLEX flow cytometer (Beckman Coulter, Inc.) with CytExpert For DxFLEX software (version 2.0.0.283; Beckman Coulter, Inc.) and analyzed using CytExpert For DxFLEX software (version 2.0.0.283; Beckman Coulter, Inc.).

Cell cycle distribution analysis. Cell cycle distribution was determined by staining DNA with PI (Beyotime Institute of Biotechnology). Briefly, cells were treated with CDDP, MG132, or CDDP + MG132 for 48 h. After treatment, cells were washed with PBS and fixed in 70% ethanol for 2 h at 4˚C. Cells were then washed again and incubated with PI staining solution at 37˚C for 30 min. The percentage of cells in the different phases of the cell cycle was measured using a DxFLEX cytometer and analyzed using CytExpert For DxFLEX software. The excitation and emission wavelengths were 488 and 617 nm.

Western blot analysis. Following treatment with CDDP and/or MG132, cells were scraped, lysed and the protein extracts were finally collected. Cell lysates were then resolved using 12% SDS-PAGE, transferred to PVDF membranes, and blocked with 5% non-fat milk in TBS-Tween 20. Subsequently, the membranes were incubated with primary antibodies against Bcl-2 (1:1,000), p53 (1:1,000; both from Abmart Pharmaceutical Technology Co., Ltd.), Bax (1:2,000; Abcepta, Inc.), or GAPDH (1:1,000; Abmart Pharmaceutical Technology Co., Ltd.) at 4˚C overnight. Following incubation with the corresponding horseradish peroxidase-conjugated goat anti-rabbit secondary antibody (1:5,000; Abmart Pharmaceutical Technology Co., Ltd.) at room temperature for 1 h, the signals were visualized using an enhanced chemiluminescence reagent (Beyotime Institute of Biotechnology) and detected using the Odyssey Fc system (LI-COR Biosciences).

Statistical analysis. Statistical analysis was performed using SPSS version 19.0 (IBM Corp.). The results were analyzed using a one-way ANOVA followed by a Tukey's post-hoc test.

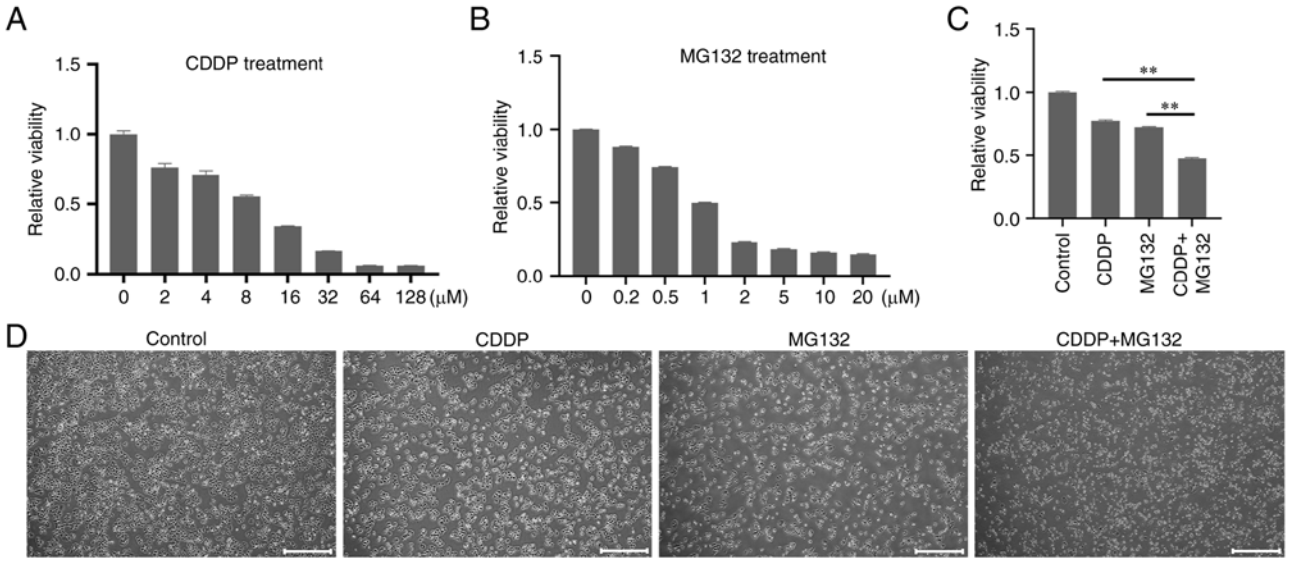

Figure 1. CDDP, MG132, or CDDP + MG132 exert inhibitory effects of oral squamous cell carcinoma cells. CAL27 cells were treated with different concentrations of (A) CDDP and (B) MG132 for 48 h after which CCK-8 assays were performed. (C) The synergistic effects of 2 μM CDDP + 0.2 μM MG132 on cell viability was assessed by CCK-8 assay. (D) Representative images showing cell morphology were captured under a light microscope. x40 magnification, scale bar 500 μm. **P<0.01. CDDP, cis-diamine-dichloroplatinum II; CCK-8, Cell Counting Kit 8.

Data are expressed as the mean ± SEM from at least three independent experiments. P≤0.05 was considered to indicate a statistically significant difference.

Results

MG132 elevates the inhibitory effect of CDDP on OSCC cell viability. To determine whether the combination of MG132 and CDDP had a synergistic anti-cancer effect, CAL27 cells were first treated with increasing concentrations of MG132 and CDDP. The results showed that cell treatment with 0.2 μM MG132 and 2 μM CDDP could significantly reduce cell viability compared with untreated control cells (Fig. 1A and B). Furthermore, 0.2 μM MG132 and 2 μM of CDDP were the minimum concentrations required to induce a significant decrease in cell viability. Therefore, these specific concentrations were used for subsequent experiments. Next, CAL27 cells were treated with 0.2 μM MG132, 2 μM CDDP, or both for 48 h. CCK-8 assays demonstrated that MG132 significantly enhanced the CDDP-induced inhibition of cell viability (Fig. 1C). Consistently, light microscopy also showed that the combined treatment synergistically enhanced cell growth inhibition compared with cell treatment with each drug alone (Fig. 1D). The above results indicated that MG132 and CDDP exerted a synergistic anti-cancer effect on OSCC.

MG132 promotes CDDP-induced ROS production and DNA damage in OSCC cells. Subsequently, to investigate whether MG132 promoted oxidative stress in OSCC cells, the intracellular ROS levels were detected in CAL27 cells using DCFH staining followed by flow cytometry. CAL27 cells were treated with MG132, CDDP, or both for 48 h and were then subjected to DCFH staining. The results showed that the intracellular ROS levels were higher in cells co-treated with CDDP and MG132 compared with cells treated with either CDDP or MG132 alone (Fig. 2A-C). Subsequently, DNA damage was assessed using a TUNEL assay. The results showed that both treatment with MG132 or CDDP alone enhanced DNA damage in OSCC cells. However, co-treatment of OSCC cells with MG132 and CDDP further promoted DNA damage (Fig. 2D and E). Overall, the above findings suggested that ROS may be involved in MG132-induced DNA damage. However, the particular mechanisms remain unclear.

MG132 enhances the inhibitory effects of CDDP on OSCC cell proliferation. It has been reported that excessive accumulation of ROS can inhibit tumor growth by inhibiting cancer cell proliferation (20). Herein, to uncover the effects of MG132 and/or CDDP on OSCC cell proliferation, a colony formation assay was performed on CAL27 cells treated with 0.2 μM MG132, 2 μM CDDP, or both for 48 h. The data demonstrated that the combination of MG132 and CDDP significantly decreased the colony formation ability of CAL27 cells compared with cells treated with either MG132 or CDDP alone (Fig. 3A and B). Furthermore, an EdU proliferation assay was performed to evaluate the proliferation ability of OSCC cells. As shown in Fig. 3C and D, MG132 combined with CDDP markedly reduced EdU staining compared with the MG132 and CDDP groups. To elucidate the mechanism of growth inhibition, cell cycle distribution experiments were performed. Compared with the untreated control cells, CDDP significantly increased the proportion of cells at sub-G1, S, and G2/M phases (P<0.01), whereas the proportion of cells in the G0/G1 phase was reduced (P<0.01), suggesting that CDDP induced cell cycle arrest in sub-G1, S, and G2/M phases in CAL27 cells. Conversely, MG132 significantly increased the proportion of cells in the G2/M phase (P<0.01) and reduced the proportion of cells in the G0/G1 phase (P<0.01), indicating that MG132 could induce G2/M arrest (Fig. 3E and F).

MG132 enhances CDDP-induced apoptosis in OSCC cells. ROS production and DNA damage are considered key

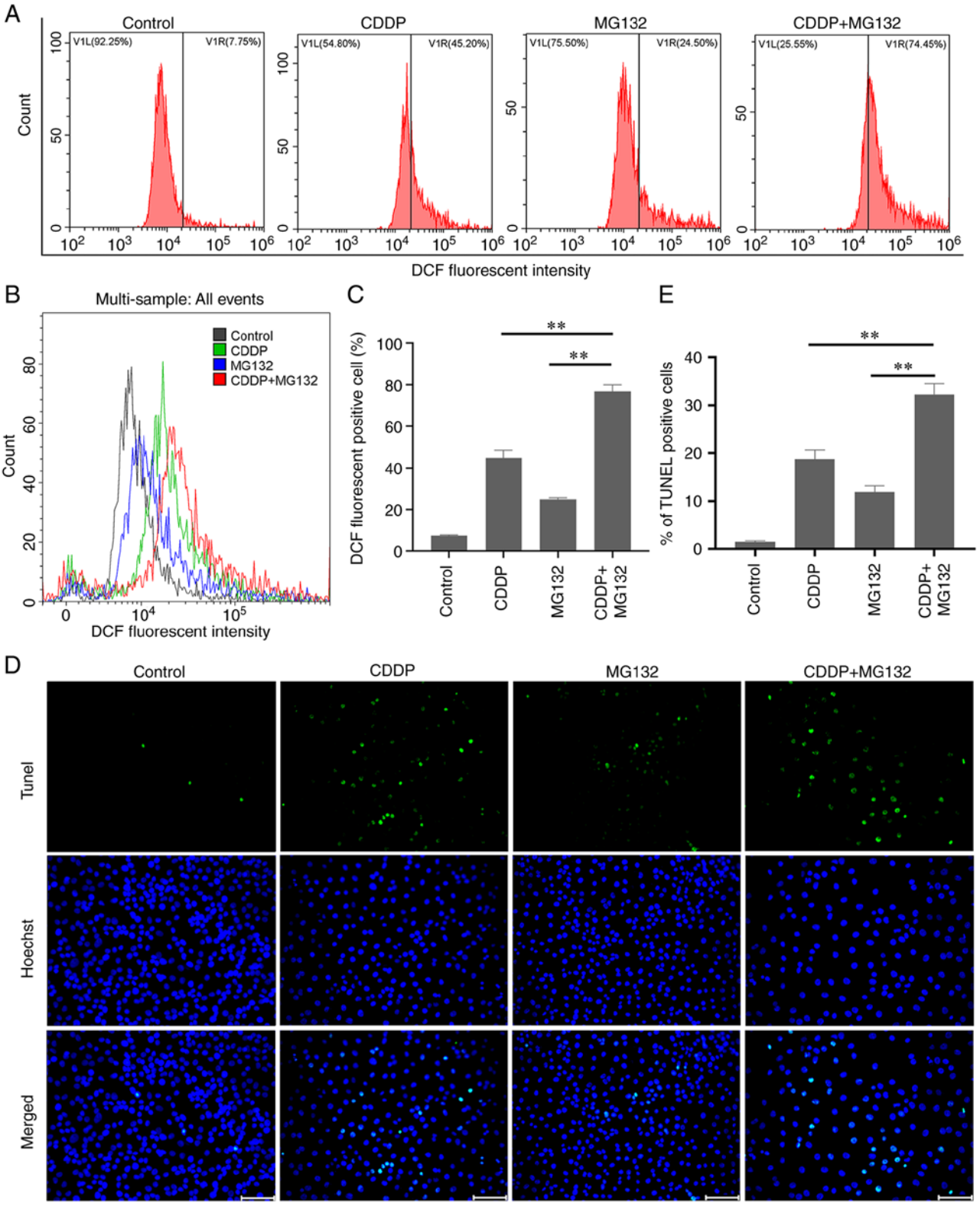

Figure 2. MG132 and CDDP synergistically enhance ROS generation and DNA damage. (A) Cells were treated with 2 μM CDDP, 0.2 μM MG132, or both together for 48 h after which intracellular ROS accumulation was assessed by flow cytometry. (B) An integrated image of (A) is shown. (C) Quantitative analysis of the percentage of DCF positive cells (n=3). (D) DNA damage was assessed by TUNEL assay under a fluorescence microscope. TUNEL staining (green) was indicative of DNA injury. Nuclei were counterstained with Hoechst (blue). x200 magnification, scale bar 100 μm. (E) Quantitative analysis of TUNEL assays was performed by measuring double TUNEL- and Hoechst-positive cells. Data are presented as the mean ± SEM from three independent experiments. **P<0.01. CDDP, cis-diamine-dichloroplatinum II; ROS, reactive oxygen species.

mechanisms involved in cell death (21). To examine whether MG132 and CDDP exerted a synergistic effect on promoting cancer cell apoptosis, double staining with V-FITC/PI was performed. Cell apoptosis was then assessed by flow cytometry. The results showed that cell treatment with CDDP or MG132 alone notably elevated cell apoptosis rate, which was

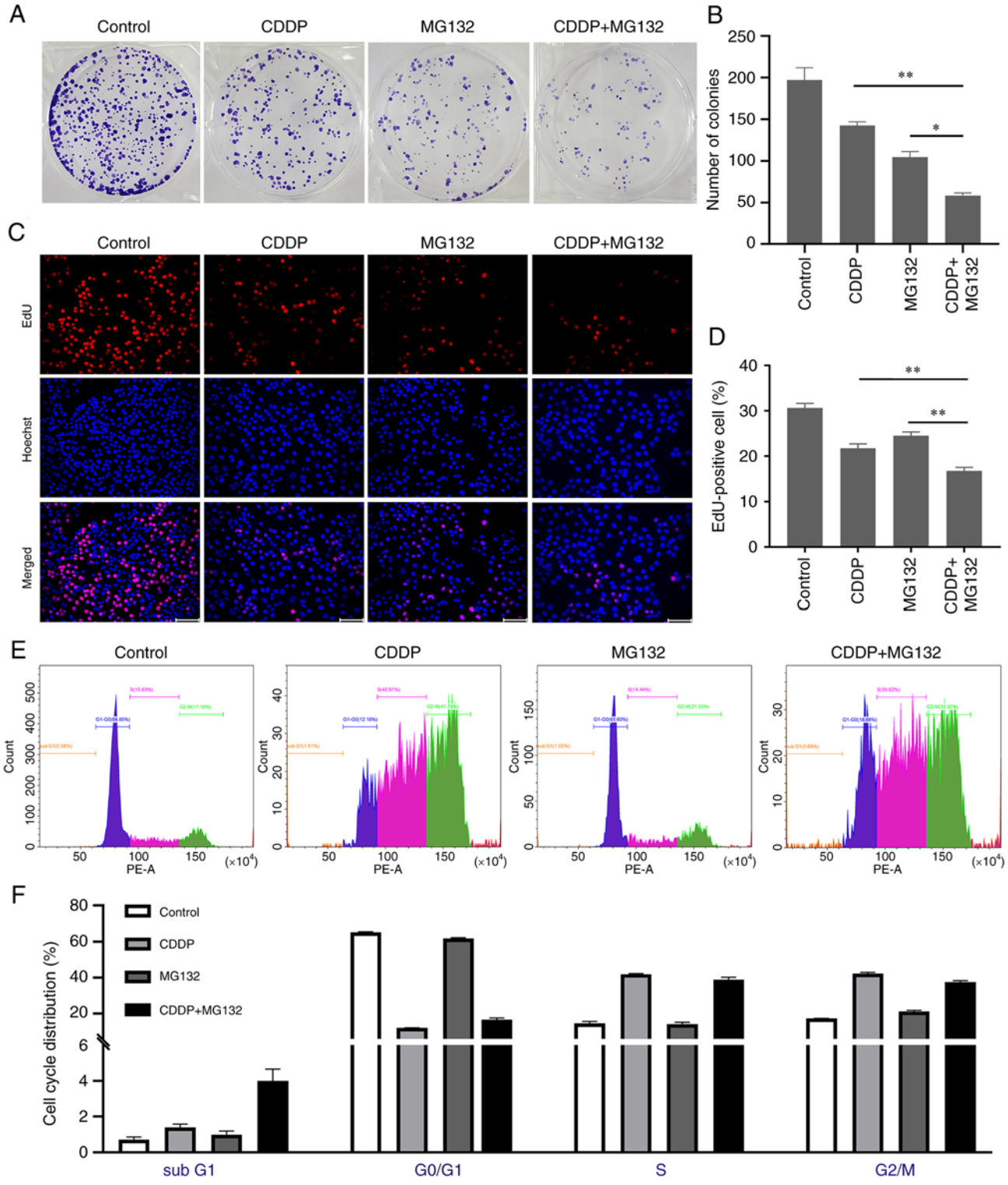

Figure 3. MG132 enhances CDDP-induced inhibition of OSCC proliferation. CAL27 cells were treated with 2 μM CDDP, 0.2 μM MG132 or both combined for 48 h. (A) Cell proliferation was assessed using colony formation assays. Representative images of colonies in a six-well-plate are shown. (B) Quantitative analysis from three independent colony formation assays are presented. (C) EdU proliferation assays were performed to determine the proliferative ability of OSCCs. Red spots indicate EdU-positive cells; cell nuclei were counterstained with Hoechst blue. x200 magnification, scale bar 100 μm. (D) Quantitative analysis of the cell proliferation ratio was performed by measuring double EdU- and Hoechst-positive cells (n=3). (E) Flow cytometry analysis for cell cycle distribution of CAL27 cells. (F) Histograms show the percentage of cells in each stage. Data are presented as the mean ± SEM of 3 independent experiments. *P<0.05 and **P<0.01. OSCC, oral squamous cell carcinoma cells; CDDP, cis-diamine-dichloroplatinum II; EdU, ethynyl-2-deoxyuridine.

further enhanced in cells co-treated with CDDP and MG132 (Fig. 4A and B). It has been reported that p53 plays a significant role in cancer cell apoptosis and regulates downstream mitochondrial apoptosis-related pathways (22). Therefore, in the current study, the expression levels of p53 and those of its downstream apoptosis-related signal pathways were determined. MG132 upregulated p53 expression and further enhanced the CDDP-induced p53 expression levels in OSCC cells (Fig. 4C).

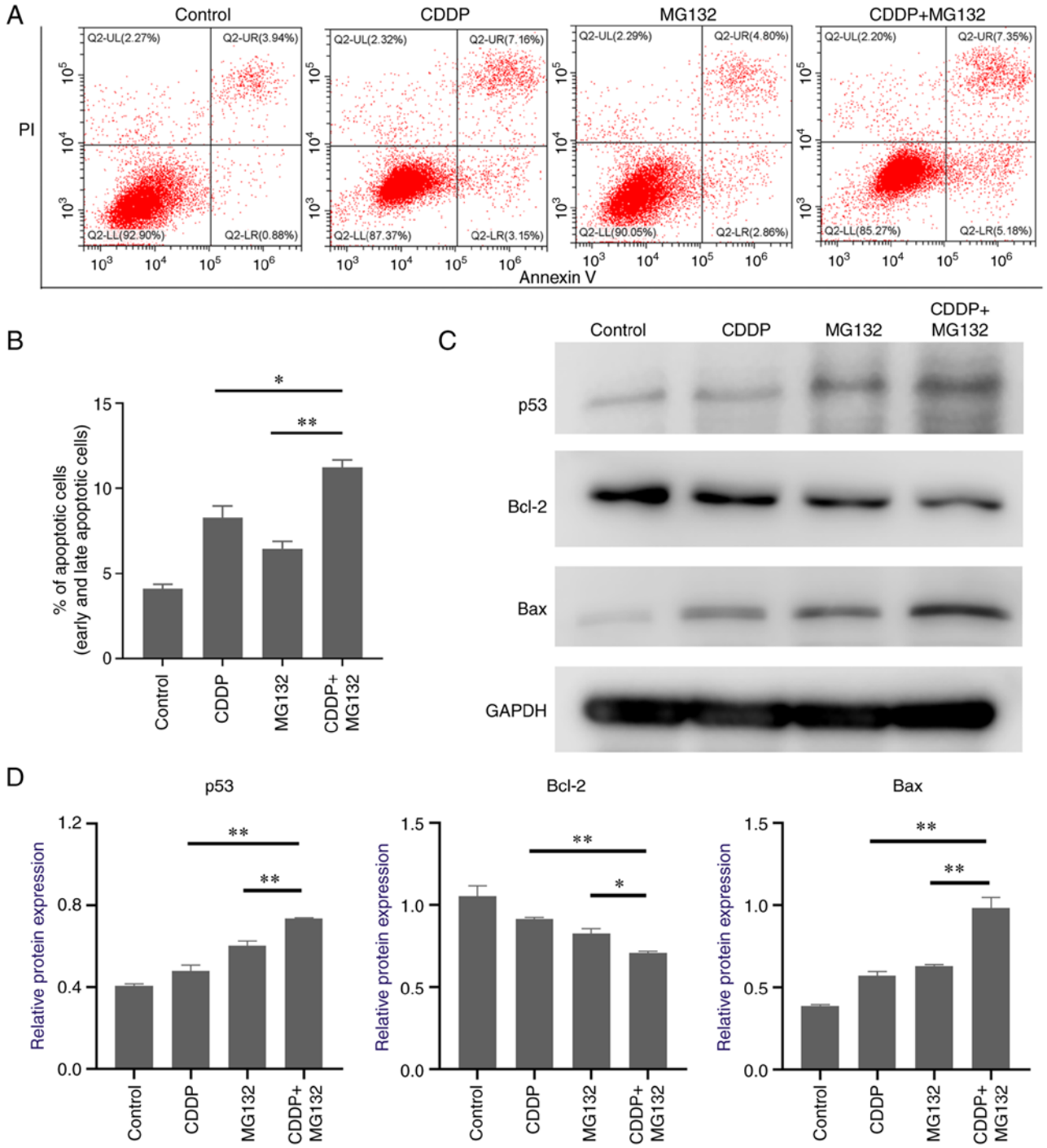

Figure 4. CDDP-induced apoptosis of oral squamous cell carcinoma cells is enhanced by MG132. (A) Representative image of flow cytometry analysis of CAL27 cells treated with CDDP, MG132, or CDDP + MG132. Cell apoptosis was assessed using an Annexin V/PI kit. Annexin V-/PI- staining indicates viable cells, Annexin V^+/PI^- early apoptotic cells, Annexin V^+/PI^+ late apoptotic cells, and Annexin V^-/PI^+ necrotic cells. (B) Quantitative analysis of total apoptotic cells (early and late apoptosis) is shown. Data are expressed as the mean ± SEM of three independent experiments. (C) Representative images of p53, Bcl-2, and Bax protein expression levels detected by western blot. (D) Densitometry analysis of the p53, Bcl-2, and Bax protein expression levels relative to GAPDH. $^*P<0.05$ and $^{**}P<0.01$. CDDP, cis-diamine-dichloroplatinum II; PI, propidium iodide.

To uncover the underlying downstream pro-apoptotic mechanisms induced by p53, the expression levels of the Bcl-2 family members were detected. As shown in Fig. 4C, Bax was markedly upregulated and Bcl-2 was significantly downregulated in cells co-treated with CDDP and MG132 compared with those treated with MG132 or CDDP alone (Fig. 4C), thus indicating that p53 and its downstream apoptosis-related genes could play a key role in MG132-induced OSCC apoptosis.

Discussion

In the majority of patients with OSCC, chemotherapeutic drugs are recommended as adjuvant therapy after surgery. CDDP is widely used as a chemotherapeutic agent for the treatment of several solid tumors. In 1978, CDDP became the first FDA-approved platinum-based compound for cancer treatment (23). Currently, CDDP, as a first-line treatment, is

the most commonly used chemotherapeutic drug for OSCC. However, the development of CDDP resistance limits its application and effectiveness. Therefore, combination therapies of CDDP with other anti-cancer drugs have been applied as novel therapeutic strategies for treating several types of cancer. The current study aimed to investigate whether combination therapy with MG132 and CDDP could reduce OSCC progression.

As a natural triterpene proteasome inhibitor derived from Chinese medicinal plants, MG132 can inhibit the proteolytic activity of the 26S proteasome complex (22,24). It has been reported that MG132 can be used to treat several types of cancer. Previous studies showed that MG132 could enhance ROS generation (25), inhibit cell proliferation (16), and promote cell apoptosis in different types of cancer (22). Additionally, the role of MG132 has been largely investigated in OSCC. Chen *et al* (26) demonstrated that MG132 could induce cell apoptosis via regulating glucose-regulated protein 78 and caspase 12 in the OSCC cell line Tca-8113. Additionally, Tsunoda *et al* (27) showed that MG132 could upregulate c-Jun in the OSCC cell lines Ca9-22 and HSC3, which in turn could form homologous dimers to enhance IL-8 expression. Other studies revealed that connective tissue growth factor upregulation (28) and deubiquitinating protein 3 downregulation (29) could both promote OSCC cell apoptosis. However, the above effect could be abolished by MG132 treatment. It has been reported that the programmed cell death (PD)-1/PD-ligand 1 (PD-L1) signaling pathway is involved in a type of tumor immune evasion strategy. Wu *et al* (30) showed that MG132 could inhibit the degradation of PD-L1 by deubiquitinating and stabilizing its protein expression in the OSCC cell lines HN4 and HN30. Furthermore, He *et al* (31) demonstrated that co-treatment of cells with metformin and 4SC-202 exerted an anti-OSCC effect by suppressing the proliferation and promoting the intrinsic apoptosis of OSCC cells both *in vitro* and *in vivo*. This study also suggested that MG132 could block the synergistic action of metformin and 4SC-202 by inhibiting the degradation of ΔNp63.

In addition to the above findings, it has also been reported that MG132 can cooperate with several genes to treat OSCC (32-34). Tumor necrosis factor (TNF)-related apoptosis-inducing ligand (TRAIL) can induce apoptosis in several types of tumor cells (35). However, resistance to TRAIL response has been verified in different types of cancer, including OSCC (34). A previous study demonstrated that MG132 enhanced TRAIL action to increase apoptosis of the OSCC cell lines HSC-2 and HSC-3 (34). In addition, MG132 could effectively cooperate with TRAIL agonists to promote OSCC cell apoptosis by stabilizing truncated Bid and Bik (33). Additionally, MG132 could synergize with short hairpin RNA against X-box-binding protein 1 to activate the inositol-requiring enzyme 1a/TNF receptor-associated factor-2/apoptosis signal-regulating kinase-1/Jun kinase pathway to promote the apoptosis of the OSCC cells, TCA8113 (32).

The present study showed that MG132 reduced OSCC cell viability in a dose-dependent manner, thus supporting its direct anti-cancer effect on OSCC. Previous studies also demonstrated that chemotherapeutic drugs combined with proteasome inhibitors improves chemotherapy sensitivity (15,16,36). However, the combination of MG132 and CDDP on OSCC has not been previously assessed. The results revealed that MG132 combined with CDDP markedly reduced cell viability compared with either MG132 or CDDP alone, thus suggesting that MG132 exhibited a synergistic effect with CDDP on OSCC cells. Previously, it has been shown that MG132 promoted neural stem cell death (37), and Bax *et al* (9) also found that MG132 negatively regulates pluripotent stem cell survival and motor neuron differentiation. The aforementioned findings indicate that the future clinical applications of MG132 may be limited. However, further studies are required to determine the toxicity and side effects of MG132 prior to clinical use.

ROS plays a crucial role in several biological processes. Maintaining ROS homeostasis is essential for the maintenance of a physiological state (9,38). Excessive ROS production often leads to oxidative stress. Under conditions of oxidative stress, excessive ROS attacks nitrogenous bases and the sugar-phosphate backbone of DNA, eventually leading to single- and double-stranded DNA breaks (39). Previous studies demonstrated that both CDDP (38) and MG132 (40) could promote ROS generation individually. The results of the present study also revealed that both CDDP and MG132 could increase ROS levels, as well as DNA damage in OSCC cells. Additionally, a synergistic effect between CDDP and MG132 on promoting ROS generation and DNA damage was observed, thus indicating that MG132 exerted an anti-cancer effect by inducing DNA damage via ROS.

Previously, the mechanisms underlying the effects of MG132 on inducing intracellular ROS generation have not been investigated. Park *et al* (41) demonstrated that the MG132-induced GSH downregulation was involved in ROS generation. In addition, the levels of O^{2-}, primarily originating from the mitochondria, were shown to be increased in MG132-treated human pulmonary fibroblast cells (42). Therefore, the particular mechanisms involved in the effects of MG132 on inducing ROS production should be addressed in future studies.

It has been reported that numerous basic biological processes, including cellular proliferation, require moderate to low ROS levels (38). Additionally, a previous study revealed that excessive ROS production overwhelms antioxidant systems, thus leading to cell cycle arrest as well as inhibition of cell proliferation (37). The current study demonstrated that the combined use of MG132 and CDDP could significantly reduce the proliferative ability of OSCC cells, as evidenced by the decreased number of cell colonies and reduced cell proliferation ratio. These findings suggested that MG132 could promote the CDDP-induced inhibition of OSCC cell proliferation by enhancing ROS production.

When ROS induces oxidative DNA damage, p53 is activated by ROS via DNA damage checkpoint pathways (23). p53 is an essential tumor suppressor factor, encoded by the tumor suppressor gene TP53. Activation of p53 is considered an attractive anti-cancer therapy approach. p53 can induce tumor cell apoptosis via regulation of its downstream mitochondrial apoptotic signaling pathway (22). Bax and Bcl-2 are both members of the Bcl-2 family. Bax promotes cell apoptosis and it is transcriptionally regulated by p53. Therefore, its expression is positively associated with p53 expression (43). By contrast, the anti-apoptotic protein Bcl-2 plays a crucial role in

cell survival. A p53-negative response element has been identified in the promoter region of Bcl-2. Therefore, it has been reported that Bcl-2 is negatively regulated by p53 (44). Here, p53 and its downstream apoptotic signaling pathways were shown to be activated in the MG132 treatment group, indicating that the MG132-induced cell apoptosis was mediated by the ROS/DNA damage/p53 axis.

In addition to the ROS/DNA damage/p53 signaling pathway, it has been also reported that MG132 can affect CDDP sensitivity in OSCC through different signaling pathways. A previous study demonstrated that MG132 inhibited the ubiquitination of phosphoglycerate kinase 1, enhance its expression, and activate the Akt/mTOR signaling pathway, eventually leading to CDDP resistance in OSCC cells (17). Additionally, another study revealed the synergistic effect of MG132 and CDDP on the SCC-25 OSCC cell line via regulation of the E-cadherin/β-catenin complex signaling pathway (18). Furthermore, minichromosome maintenance deficient 5 (MCM5) promoted DNA repair in OSCC cells via interacting with long non-coding RNA POP1-1, thus resulting in the onset of resistance in OSCC cells. MG132 could also significantly downregulate MCM5 in OSCC cells, thus suggesting that MG132 could inhibit CDDP resistance (19).

In conclusion, the present study demonstrated that MG132 affected the behavior of OSCC cells by inhibiting cell growth and triggering cell apoptosis. In addition to the inhibitory effect of MG132 alone, a synergistic effect was also revealed in cells co-treated with CDDP and MG132 via the ROS/DNA damage/p53 axis. The above findings supported the clinical application of MG132 as an effective adjuvant with CDDP in the management of OSCC.

Acknowledgements

The authors would like to thank Professor Zhiyong Wang (Nanjing Stomatological Hospital, Nanjing, China) for providing the CAL27 OSCC cell line.

Funding

The current work was supported by funding from Nantong Science and Technology Bureau (Nantong, China; grant no. MS12020032).

Availability of data and materials

The datasets used and/or analyzed during the current study are available from the corresponding author on reasonable request.

Authors' contributions

ZZ wrote the first draft of the manuscript and performed the experiments. XW designed the study and analyzed data. DC designed the study, revised the manuscript, and obtained the funding. All authors have read and approved the final manuscript, and confirm the authenticity of all the raw data.

Ethics approval and consent to participate

Not applicable.

Patient consent for publication

Not applicable.

Competing interests

The authors declare that they have no competing interests.

References

1. Warnakulasuriya S and Kerr AR: Oral cancer screening: Past, present, and future. J Dent Res 100: 1313-1320, 2021.
2. Papa F, Siciliano RA, Inchingolo F, Mazzeo MF, Scacco S and Lippolis R: Proteomics pattern associated with gingival oral squamous cell carcinoma and epulis: A case analysis. Oral Sci Int 15: 41-47, 2018.
3. Mohapatra P, Shriwas O, Mohanty S, Ghosh A, Smita S, Kaushik SR, Arya R, Rath R, Das Majumdar SK, Muduly DK, *et al*: CMTM6 drives cisplatin resistance by regulating Wnt signaling through the ENO-1/AKT/GSK3β axis. JCI Insight 6: e143643, 2021.
4. Huang SH and O'Sullivan B: Oral cancer: Current role of radiotherapy and chemotherapy. Med Oral Patol Oral Cir Bucal 18: e233-e240, 2013.
5. Kulkarni B, Gondaliya P, Kirave P, Rawal R, Jain A, Garg R and Kalia K: Exosome-mediated delivery of miR-30a sensitize cisplatin-resistant variant of oral squamous carcinoma cells via modulating Beclin1 and Bcl2. Oncotarget 11: 1832-1845, 2020.
6. Yuan Y, Xie X, Jiang Y, Wei Z, Wang P, Chen F, Li X, Sun C, Zhao H, Zeng X, *et al*: LRP6 is identified as a potential prognostic marker for oral squamous cell carcinoma via MALDI-IMS. Cell Death Dis 8: e3035, 2017.
7. Bassermann F, Eichner R and Pagano M: The ubiquitin proteasome system-implications for cell cycle control and the targeted treatment of cancer. Biochim Biophys Acta 1843: 150-162, 2014.
8. Gupta I, Singh K, Varshney NK and Khan S: Delineating crosstalk mechanisms of the ubiquitin proteasome system that regulate apoptosis. Front Cell Dev Biol 6: 11, 2018.
9. Bax M, McKenna J, Do-Ha D, Stevens CH, Higginbottom S, Balez R, Cabral-da-Silva MEC, Farrawell NE, Engel M, Poronnik P, *et al*: The ubiquitin proteasome system is a key regulator of pluripotent stem cell survival and motor neuron differentiation. Cells 8: 581, 2019.
10. Narayanan S, Cai CY, Assaraf YG, Guo HQ, Cui Q, Wei L, Huang JJ, Ashby CR Jr and Chen ZS: Targeting the ubiquitin-proteasome pathway to overcome anti-cancer drug resistance. Drug Resist Updat 48: 100663, 2020.
11. Yang H, Chen X, Li K, Cheaito H, Yang Q, Wu G, Liu J and Dou QP: Repurposing old drugs as new inhibitors of the ubiquitin-proteasome pathway for cancer treatment. Semin Cancer Biol 68: 105-122, 2021.
12. Guo N and Peng Z: MG132, a proteasome inhibitor, induces apoptosis in tumor cells. Asia Pac J Clin Oncol 9: 6-11, 2013.
13. Zhu W, Liu J, Nie J, Sheng W, Cao H, Shen W, Dong A, Zhou J, Jiao Y, Zhang S and Cao J: MG132 enhances the radiosensitivity of lung cancer cells *in vitro* and *in vivo*. Oncol Rep 34: 2083-2089, 2015.
14. Qiang W, Sui F, Ma J, Li X, Ren X, Shao Y, Liu J, Guan H, Shi B and Hou P: Proteasome inhibitor MG132 induces thyroid cancer cell apoptosis by modulating the activity of transcription factor FOXO3a. Endocrine 56: 98-108, 2017.
15. Guo N, Peng Z and Zhang J: Proteasome inhibitor MG132 enhances sensitivity to cisplatin on ovarian carcinoma cells in vitro and in vivo. Int J Gynecol Cancer 26: 839-844, 2016.
16. Dang L, Wen F, Yang Y, Liu D, Wu K, Qi Y, Li X, Zhao J, Zhu D, Zhang C and Zhao S: Proteasome inhibitor MG132 inhibits the proliferation and promotes the cisplatin-induced apoptosis of human esophageal squamous cell carcinoma cells. Int J Mol Med 33: 1083-1088, 2014.
17. Jiang Q, Wang Z, Qi Q, Li J, Xin Y and Qiu J: lncRNA SNHG26 promoted the growth, metastasis, and cisplatin resistance of tongue squamous cell carcinoma through PGK1/Akt/mTOR signal pathway. Mol Ther Oncolytics 24: 355-370, 2022.
18. Lü L, Liu X, Wang C, Hu F, Wang J and Huang H: Dissociation of E-cadherin/β-catenin complex by MG132 and bortezomib enhances CDDP induced cell death in oral cancer SCC-25 cells. Toxicol In Vitro 29: 1965-1976, 2015.

19. Jiang Y, Guo H, Tong T, Xie F, Qin X, Wang X, Chen W and Zhang J: lncRNA lnc-POP1-1 upregulated by VN1R5 promotes cisplatin resistance in head and neck squamous cell carcinoma through interaction with MCM5. Mol Ther 30: 448-467, 2022.
20. Huang R, Chen H, Liang J, Li Y, Yang J, Luo C, Tang Y, Ding Y, Liu X, Yuan Q, *et al*: Dual role of reactive oxygen species and their application in cancer therapy. J Cancer 12: 5543-5561, 2021.
21. Srinivas US, Tan BWQ, Vellayappan BA and Jeyasekharan AD: ROS and the DNA damage response in cancer. Redox Biol 25: 101084, 2019.
22. Aubrey BJ, Kelly GL, Janic A, Herold MJ and Strasser A: How does p53 induce apoptosis and how does this relate to p53-mediated tumour suppression? Cell Death Differ 25: 104-113, 2018.
23. Baruah A, Chang H, Hall M, Yuan J, Gordon S, Johnson E, Shtessel LL, Yee C, Hekimi S, Derry WB and Lee SS: CEP-1, the Caenorhabditis elegans p53 homolog, mediates opposing longevity outcomes in mitochondrial electron transport chain mutants. PLoS Genet 10: e1004097, 2014.
24. Gonzalez-Campora R, Davalos-Casanova G, Beato-Moreno A, Garcia-Escudero A, Pareja Megia MJ, Montironi R and Lopez-Beltran A: BCL-2, TP53 and BAX protein expression in superficial urothelial bladder carcinoma. Cancer Lett 250: 292-299, 2007.
25. Han YH, Moon HJ, You BR and Park WH: The effect of MG132, a proteasome inhibitor on HeLa cells in relation to cell growth, reactive oxygen species and GSH. Oncol Rep 22: 215-221, 2009.
26. Chen SF, Chen HY, Liu XB, Zhang YX, Liu W, Wang WH, Zhang B and Wang LX: Apoptotic effect of MG-132 on human tongue squamous cell carcinoma. Biomed Pharmacother 65: 322-327, 2011.
27. Tsunoda M, Fukasawa M, Nishihara A, Takada L and Asano M: JunB can enhance the transcription of IL-8 in oral squamous cell carcinoma. J Cell Physiol 236: 309-317, 2021.
28. Lai WT, Li YJ, Wu SB, Yang CN, Wu TS, Wei YH and Deng YT: Connective tissue growth factor decreases mitochondrial metabolism through ubiquitin-mediated degradation of mitochondrial transcription factor A in oral squamous cell carcinoma. J Formos Med Assoc 117: 212-219, 2018.
29. Luo F, Zhou Z, Cai J and Du W: DUB3 facilitates growth and inhibits apoptosis through enhancing expression of EZH2 in oral squamous cell carcinoma. Onco Targets Ther 13: 1447-1460, 2020.
30. Wu J, Guo W, Wen D, Hou G, Zhou A and Wu W: Deubiquitination and stabilization of programmed cell death ligand 1 by ubiquitin-specific peptidase 9, X-linked in oral squamous cell carcinoma. Cancer Med 7: 4004-4011, 2018.
31. He Y, Tai S, Deng M, Fan Z, Ping F, He L, Zhang C, Huang Y and Cheng B: Metformin and 4SC-202 synergistically promote intrinsic cell apoptosis by accelerating ΔNp63 ubiquitination and degradation in oral squamous cell carcinoma. Cancer Med 8: 3479-3490, 2019.
32. Chen H, Yang H, Pan L, Wang W, Liu X, Ren X, Liu Y, Liu W, Zhang Y, Jiang L, *et al*: The molecular mechanisms of XBP-1 gene silencing on IRE1α-TRAF2-ASK1-JNK pathways in oral squamous cell carcinoma under endoplasmic reticulum stress. Biomed Pharmacother 77: 108-113, 2016.
33. Sung ES, Park KJ, Choi HJ, Kim CH and Kim YS: The proteasome inhibitor MG132 potentiates TRAIL receptor agonist-induced apoptosis by stabilizing tBid and Bik in human head and neck squamous cell carcinoma cells. Exp Cell Res 318: 1564-1576, 2012.
34. Yoshiba S, Iwase M, Kurihara S, Uchida M, Kurihara Y, Watanabe H and Shintani S: Proteasome inhibitor sensitizes oral squamous cell carcinoma cells to TRAIL-mediated apoptosis. Oncol Rep 25: 645-652, 2011.
35. Deng D and Shah K: TRAIL of hope meeting resistance in cancer. Trends Cancer 6: 989-1001, 2020.
36. Zhang Y, Yang B, Zhao J, Li X, Zhang L and Zhai Z: Proteasome inhibitor Carbobenzoxy-L-Leucyl-L-Leucyl-L-Leucinal (MG132) enhances therapeutic effect of paclitaxel on breast cancer by inhibiting nuclear factor (NF)-κB signaling. Med Sci Monit 24: 294-304, 2018.
37. Kim YM and Kim HJ: Proteasome inhibitor MG132 is toxic and inhibits the proliferation of rat neural stem cells but increases BDNF expression to protect neurons. Biomolecules 10: 1507, 2020.
38. Kleih M, Böpple K, Dong M, Gaißler A, Heine S, Olayioye MA, Aulitzky WE and Essmann F: Direct impact of cisplatin on mitochondria induces ROS production that dictates cell fate of ovarian cancer cells. Cell Death Dis 10: 851, 2019.
39. Han YH, Kim SZ, Kim SH and Park WH: Reactive oxygen species and glutathione level changes by a proteasome inhibitor, MG132, partially affect calf pulmonary arterial endothelial cell death. Drug Chem Toxicol 33: 403-409, 2010.
40. Han YH, Moon HJ, You BR and Park WH: The attenuation of MG132, a proteasome inhibitor, induced A549 lung cancer cell death by p38 inhibitor in ROS-independent manner. Oncol Res 18: 315-322, 2010.
41. Park S, Park JA, Yoo H, Park HB and Lee Y: Proteasome inhibitor-induced cleavage of HSP90 is mediated by ROS generation and caspase 10-activation in human leukemic cells. Redox Biol 13: 470-476, 2017.
42. Park WH and Kim SH: MG132, a proteasome inhibitor, induces human pulmonary fibroblast cell death via increasing ROS levels and GSH depletion. Oncol Rep 27: 1284-1291, 2012.
43. Miyashita T, Krajewski S, Krajewska M, Wang HG, Lin HK, Liebermann DA, Hoffman B and Reed JC: Tumor suppressor p53 is a regulator of bcl-2 and bax gene expression in vitro and in vivo. Oncogene 9: 1799-1805, 1994.
44. Zhang Y, Zhang Y, Zhong C and Xiao F: Cr(VI) induces premature senescence through ROS-mediated p53 pathway in L-02 hepatocytes. Sci Rep 6: 34578, 2016.